Vol. 20, No. 1 (2021) 25-36
Revista Mexicana de Ingeniería Química

1-D coordination polymer with helical chirality in octacyanomolybdate (V)- and Nd(III)-based: Synthesis, structure, and Hirshfeld surface analyses

Polímero de coordinación 1-D con quiralidad helicoidal basado en octacianomolibdato (V)- y Nd(III): Síntesis, estructura y análisis de superficie de Hirshfeld

Mohd. Muddassir*

Department of Chemistry, College of Science, King Saud University, Riyadh 11451.

Received: March 19, 2020; Accepted: April 23, 2020

Abstract

A new 1-D cyanide-based coordination polymer consisting of octacyanomolybdate(V) and Nd(III) has been synthesized and characterized through a single-crystal X-ray and elemental analysis. The compound consists of 1-D chains single strand chiral helix of $[(Terpy)(DMF)_3(MeOH)Nd\text{-}CN\text{-}Mo(CN)_7]$ (NdMo-1) (Terpy is 2,2':6',2"-terpyridine, DMF is dimethylformamide), where each $Mo^{V}(CN)_8^{3-}$ entity acts as a two-monodentate bridging ligand towards two Nd(III) ions through two of its eight cyanide groups in cis positions, respectively, in an alternating fashion. Corresponding chains are connected utilizing hydrogen bond interactions to form a three-dimensional supramolecular structure that stabilizes the whole molecule. These interactions have been validated using the Hirshfeld surface analysis.

Keywords: Octacyanomolybdate(V), X-ray crystallography, chiral helicity, H-bonding,Hirshfeld analyses.

Resumen

Se sintetizó y caracterizó un nuevo polímero que consiste en octacianomolibdato(V) y Nd(III) a través de un análisis de rayos X de cristal sencillo y elemental. El compuesto consiste de cadenas 1-D de hélice quiral en filamentos sencillos de $[(Terpy)(DMF)_3(MeOH)Nd\text{-}CN\text{-}Mo(CN)_7]$ (NdMo-1) (Terpy es 2,2':6',2"-terpiridina, DMF es dimetilformamida), donde cada entidad de $Mo^{V}(CN)_8^{3-}$ actúa como un ligando de puente de dos-monodentados hacia dos iones Nd(II) a través de dos de sus seis grupos ciano en posiciones cis, respctivamente, en una forma alternada. Las cadenas correspondientes están conectadas usando interacciones de enlaces de hidrógeno para formar una estructura tridimensional we estabiliza a toda la molécula. Estas interacciones han sido validades a partir de análisis superficial de Hirshfeld.

Palabras clave: Octacianomolibdato (V), cristalografía de rayos-X, hilicidad quiral, enlace-H, análisis de Hirshfeld.

1 Introduction

Cyanide-based materials are broadly utilized in various fields, for instance, coordination chemistry, especially in the synthesis of molecular magnets because of their high electric charge density on both donor atoms (Goodwin *et al*., 2008; Kaye & Long, 2005; Ohkoshi, *et al*., 2011; Qian *et al*., 2011; Sato *et al*., 1996; J. Wang *et al*., 2010, p. 3101; X.-Y. Wang *et al*., 2010; Yuan *et al*., 2010). However, there are certain limitations associated with the cyanide group such as its strong coordinating ability that causes the reacting products to precipitate immediately during synthesis owing to the formation of multidimensional cyanide-based polymer materials. Further, studies related to their applications were obstructed owing to the absence of well-shaped single crystals suitable for physical measurements (Z.-X. Wang *et al*., 2006). These drawbacks can be overcome by introducing additional small ligands in the synthesis of cyanide-based complexes as the small ligands can control the growth of the crystal by maintaining competition between coordination and precipitation such that it ultimately results in obtaining the desired crystalline materials bearing polycyanide groups and accessing its structure quickly (Chelebaeva *et al*., 2009, 2008; Ma *et al*., 2009; Ma *et al*., 2010; Prins *et al*., 2007; Tanase *et al*., 2008). Several cyanide-based ligands can act as building blocks for the preparation of these crystalline materials.

* *Corresponding author. E-mail*: mmohammadarshad@ksu.edu.sa, muddassirchem@gmail.com
https://doi.org/10.24275/rmiq/Poli1474
issn-e: 2395-8472

Among them, the octacyanometalate building block can generate cyano-bridged heterobimetallic systems that display all possible dimensionalities (Chorazy *et al*., 2014; Gao *et al*., 2018; Tanase *et al*., 2011). The prediction of the rich topology of polynuclear systems based on octacyanometalates is still a challenge. Despite this, a possible way to understand the formation of extended architectures is based on the preference given to specific geometries of cationic building blocks. Essentially, the geometry and number of the labile coordination sites present at the cationic building block is the main aspect. However, there are more subtle effects (solvents, counterions, competition between solvent and cyano-bridging in the substitution reaction, etc.) that influence the final topology (Chorazy *et al*., 2018; Nowicka *et al*., 2012; Prins *et al*., 2007; Tanase *et al*., 2011). Several studies have led to the realization of the multifunctionality of the octacyanometalate-based molecular materials. The most promising assemblies from the viewpoint of potential applications in modern nanotechnology are high spin polynuclear clusters, molecules displaying spin reorientation phenomena, and the extended coordination networks combining optical and magnetic properties (Chorazy *et al*., 2017; Hendrickx *et al*., 2004). Several complexes of the octacyanometalate-based complexes were prepared with first- and second-row transition metal ions that exhibited intriguing properties. Compared to 3d−4d metal complexes in combination with octacyanometalates, the homo- and heterometallic coordination networks based on lanthanide centers such as 4d−4f offer attractive properties in terms of their material properties and potential applications in data storage, quantum computing, or nonlinear optics (Chorazy *et al*., 2016; Chorazy *et al*., 2017; Shen, 2014; Z.-X. Wang, Shen, *et al*., 2006). Discrete polynuclear 4d−4f electron systems are of significant interest from the viewpoint of single-molecule-magnet construction and material chemistry because of both large-spin and considerable single-ion anisotropy provided by it. The rational design of f−d cyano-bridged architectures tuned by the lanthanide center attracts considerable attention in the field of functional magnetic materials. The exploration of cyano-bridged 4f−4d systems resulted in a wide variety of coordination networks from ionic compounds and discrete molecules, through 1-D chains and two-dimensional (2-D) layers to three-dimensional (3-D) Prussian blue analogs (Chorazy *et al*., 2014; Gao *et al*., 2018; Prins *et al*., 2007).

Chirality is a fundamental property of a molecule in which it is non-superimposable to its mirror image. The coordination predilection of the metal ions to the ligand and its coordination number can give an interesting chiral topology. The structural feature of a ligand is one of the factors that can favor molecular architecture. Molecular tectonics, an approach used to buildup chiral topology of molecules using self-assembly of different molecular building blocks, which are complementary with each other (Kaes *et al*., 1998). Here, we utilized coordination of two metals Mo (V) and Nd (III) with an aromatic ligand to create a helical topology which is non-superimposable to each other. Therefore, we synthesized a helically chiral metal coordinated polymer in solid-state with the help of the various non-covalent interactions of aromatic ligands.

Wong *et al*. reported that the presence of ligands with aromatic groups leads to the formation of the $\pi - \pi$ stacking interactions between clusters, while the lattice solvent molecules such as water or methanol form hydrogen-bonding interactions (Z.-X. Wang, Zhang, *et al*., 2006). It was further reported that this prevents the observation of single-molecule magnetic behavior in these complexes despite their frequency dependence in ac magnetic measurements. Similarly, Song *et al*. have demonstrated that no out-of-phase signals were observed in the AC magnetic susceptibilities for complexes synthesized by lanthanides [Dy(III), Ho(III)], $K_3M(CN)_6$ [M= Fe(III), Co(III)] and similar terpyridine complexes. Interestingly, in the case of the Dy(III), a 1-D chain is formed, while in the case of Ho(III), a rectangular molecular structure is formed as [2+2] owing to the ionic radii contraction of the lanthanides(Muddassir *et al*., 2013).

Given these considerations, we have decided to synthesize 4d−4f cyano-bridged assemblies using $Mo(CN)_8^{3-}$ ion as a building block and structurally characterized a 1-D polymer chain of $[(Terpy)(DMF)_3(MeOH)Nd\text{-}CN\text{-}Mo(CN)_7]$ by single-crystal XRD. Terpyridine was chosen as a blocking ligand because it can block the coordination sites of the metal and hence limit the dimension of the molecules rather than the extended network as it is reported in the literature that ligand selection is crucial for synthesizing these kinds of heterometallic complexes.

2 Materials and methods

2.1 Physical Measurement

2.1.1 Starting Materials

Chemicals such as $Nd(NO_3)_3{\cdot}6H_2O$ (99.9% trace metals basis), 2,2':6',2"-terpyridine (98%) and solvents (anhydrous, 99.8%) were purchased from Sigma-Aldrich and utilized as received without further purification. $Cs_3[Mo(CN)_8]{\cdot}4H_2O$ was prepared according to a previously reported literature (Bok *et al*., 1975).

Caution! *Cyanides are hyper-toxic and hazardous, and thus should be handled in small quantities and with great caution!*

2.1.2 Methods and instrumentation

Microanalysis (CHN) was carried out with a Carlo Erba Analyzer Model 1108.

2.1.3 Synthesis

Here, we describe the synthesis of [(Terpy)$(DMF)_3$(Me OH)Nd-CN-$Mo(CN)_7$], hereafter referred to as Complex NdMo-1 .

A solution of $Nd(NO_3)_3{\cdot}6H_2O$ (43.8 mg, 0.1 mmol) and terpy (23.3 mg, 0.1 mmol) were dissolved in MeOH (10 mL) and stirred for 30 min followed by the dropwise addition of $Cs_3[Mo(CN)_8]{\cdot}4H_2O$ (78.5 mg, 0.1 mmol) in H_2O (8 mL) with continuous stirring. The resulting yellow precipitate was dissolved using DMF (2.5 mL). The resulting mixture was allowed to stand undisturbed in the dark for three weeks and yellow block-shaped single crystals of Complex NdMo-1 suitable for X-ray analysis were obtained (yield 38%). Elemental analysis for $C_{34}H_{36}MoN_{14}NdO_5$: C 42.50, H 3.78, N 20.41%; found: C 43.40, H 3.96, N 20.90%.

2.2 Crystal structure determination

Single crystals of Complex NdMo-1 were coated with a trace of Fomblin oil and quickly transferred to the goniometer head of a Bruker Quest diffractometer with a fixed chi angle, a sealed tube fine focus X-ray tube, a single crystal curved graphite incident beam monochromator, a Photon100 CMOS area detector, and an Oxford Cryosystems low-temperature device. Examination and data collection were performed with Mo Kα radiation (λ = 0.71073 Å) at 150 K.

Data reduction and unit cell refinement for NdMo-1 was performed using SAINT-Plus (SAINT, 2014). The SHELXL-2014/7 (G M Sheldrick, 2008; George M Sheldrick, 2015) software was used to solve the structure of NdMo-1 by the direct method and refined by full-matrix least-squares against F2 with all the reflections. All non-hydrogen atoms were refined anisotropically. Hydrogen atoms were placed onto calculated positions and refined using a riding model. The structure had been a merohedral twinning in it. The twin matrix corresponds to an inverted symmetry here with the reported twinning factor comparable to the Flack parameter. The inverted symmetry reported for the crystal structure presented in this investigation corresponds to the operation of non-centrosymmetric space group with Laue group of operation.

2.3 Hirshfeld surface analyses

The Hirshfeld surfaces for the complex have been generated by using Crystal Explorer 3.1 software and are mapped with d_{norm} and 2D fingerprint plots of d_e with d_i (Yadav *et al*., 2015). All the Hirshfeld plots are constructed by considering the disorder in the molecule (He *et al*., 2019; Kumar *et al*., 2013). All the Hirshfeld surfaces have been plotted in transparent mode to allow the visualization of the atom centers in the molecular framework.

3 Results and discussion

The yellow block-shaped crystals of Complex NdMo-1 were obtained in moderate yield. The acquired complex is stable towards air and moisture.

3.1 Single crystal X-Ray structure analysis

The complex NdMo-1 crystallizes in an orthorhombic crystal system with *Pca21* space group. The structural analysis reveals that the compound is a 1-D coordination polymer having $Mo^V(CN)_8$ unit bridged between two neodymium centers; cyanide ligand being an ambidentate ligand coordinates with the soft center molybdenum atom through carbon linkages while comparatively harder neodymium center (due to lanthanide contraction and relativistic effects) coordinates with hard the nitrogen atom.

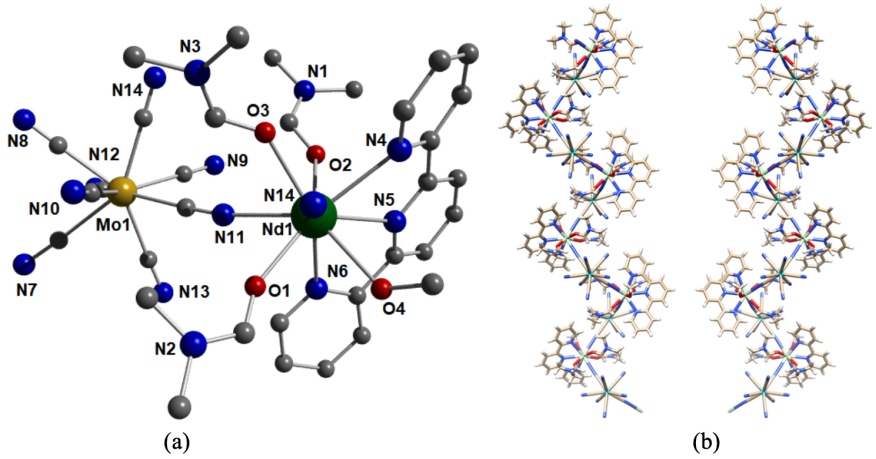

Fig. 1. (a) Perspective view of Complex NdMo-1. Hydrogen atoms and lattice MeOH have been omitted for clarity. (Color code: Green-Neodymium, Orange-Molybdenum, Blue-Nitrogen, Grey-Carbon, and Red-Oxygen). (b) Helical structure of the complex NdMo-1 with its mirror-image.

Table 1. Crystal data and structure refinement for Complex NdMo-1.

CCDC No.	**1978090**
Empirical formula	$C_{34}H_{36}MoN_{14}NdO_5$
Formula weight	l
Temperature	296(2) K
Wavelength	0.71073 Å
Crystal system	orthorhombic
Space group	*Pca21*
Unit cell dimensions	a = 24.264(3) Å α= 90° b = 10.2056(12) Å β= 90° c = 16.1495(18) Å γ = 90°
Volume	3999.1(8) $Å^3$
Z	4
Density (calculated)	1.594 Mg/m^3
Absorption coefficient	1.655 mm^{-1}
F(000)	1916
Crystal size	0.09 x 0.11 x 0.13 mm^3
Theta range for data collection	2.506 to 27.565°
Index ranges	-29≤h≤30, -9≤k≤12, -19≤l≤20
Reflections collected	8072
Independent reflections	7926 [R(int) = 0.0204]
Completeness to theta = 27.565°	99%
Absorption correction	Multi-scan
Max. and min. transmission	0.7456 and 0.5239
Refinement method	Full-matrix least-squares on F2
Data / restraints / parameters	8072/1/504
Goodness-of-fit on F2	1.074
Final R indices [I>2sigma(I)]	R1 = 0.0200, wR2 = 0.0497
R indices (all data)	R1 = 0.0204, wR2 = 0.0499
Extinction coefficient	n/a
Largest diff. peak and hole	1.313 and -0.496 $e.Å^{-3}$

Table 2. List of selected bond distances (Å) and bond angles (°) for Complex NdMo-1.

Nd(1)-O(2) 2.386(3)	Mo(1)-C(27) 2.156(4)
Nd(1)-O(3) 2.416(3)	Mo(1)-C(26) 2.160(5)
Nd(1)-O(1) 2.487(3)	Mo(1)-C(29) 2.162(5)
Nd(1)-O(4) 2.517(3)	Mo(1)-C(32) 2.167(4)
Nd(1)-N(11) 2.621(4)	Mo(1)-C(28) 2.169(5)
Nd(1)-N(6) 2.631(4)	Mo(1)-C(31) 2.170(5)
Nd(1)-N(4) 2.635(4)	Mo(1)-C(33) 2.170(4)
Nd(1)-N(14) 2.645(4)	Mo(1)-C(30) 2.174(4)
N(4)-C(15) 1.357(6)	N(14)-C(33) 1.141(6)
N(8)-C(27) 1.150(6)	N(9)-C(28) 1.132(6)
N(13)-C(31) 1.147(6)	N(2)-C(4) 1.303(6)
C(26)-N(7) 1.143(6)	N(11)-C(30) 1.146(6)
C30-N11-Nd1 170.1 (2)	N8-C27-Mo1 179.0(3)
C1-O1-Nd1 136.7 (2)	N11-C30-Mo1 176.9 (3)
C20-N5-Nd1 121.2 (2)	N7-C26-Mo1 178.1 (3)
C16-N5-Nd1 118.6 (19)	N9-C28-Mo1 177.8 (3)
C7-O3-Nd1 138.0 (2)	N14-C33-Mo1 177.0 (3)
C4-O2-Nd1 153.9 (2)	N13-C31-Mo1 179.7 (3)
C33-N14-Nd1ii 172.8 (2)	N12-C32-Mo1 178.1 (3)
C10-O4-Nd1 128.0 (2)	N10-C29-Mo1 178.4 (3)
C25-N6-Nd1 119.76 (19)	
C21-N6-Nd1 121.6 (2)	
C15-N4-Nd1 118.80 (19)	
C11-N4-Nd1 121.2 (2)	

The crystallographic data, selected bond lengths, and bond angles are listed in Table 1. The neodymium atom is nine-coordinated where three coordination sites are occupied with nitrogen atoms of the terpyridine molecule, two sites are occupied with nitrogen atoms of the cyanide ligand, three DMF solvent molecules coordinate through oxygen atoms at three different sites and another site is coordinated by the oxygen atom of methanol solvent (Figure 1a).

It is interesting to note that the Mo(V) ion only coordinated with cyanide and Nd(III) attached with the aromatic ligand and DMF molecules. These two units are assembled through cyanide bridge in a cis fashion, which is responsible for the backbone of the architecture (Figure 1b). The angles between bridged cyanides with Mo(V) and Nd(III) are 120.32 and 137.39, respectively. These angles play a crucial role in axial elongation of these units alternatively fashion to get a 1-D polymer. Unlike DNA, it is a single strand helix. The found helix from X-ray crystallography is clockwise rotatable (P configuration) and shown in Figure 1b (left side), and the mirror image of it is given on the right side of the same figure.

The geometry around the Mo^{V} center in $Mo^{V}(CN)_8$ slightly distorted square anti-prism where the cyano nitrogens N7, N8, N12, and N13 forms one plane while N9, N10, N11, and N14 is forming another plane of the square-antiprism. The separation between the two planes is 3.52 Å. Out of the eight cyano groups, the two cyano groups (C30N11 and C33N14) behave like the bridging ligand connecting the two neighboring Nd(III) centers in a cisoid mode, while rest of the six cyano ligands are terminal in nature. The Mo−CN bond lengths range from 2.156(4)-2.146(4) Å, and the C≡N bond lengths range from 1.141(6)-1.463(7) Å. Mo−C≡N linkages are almost linear, with the angles ranging from 176.1(7)-179.7(4)º. The Mo−CN bond lengths range from 2.156(4) to 2.174(4) Å, the C≡N bond lengths range from 1.131(6) to 1.463(7) Å. All the bond lengths are almost comparable to those of similar complexes reported in the literature [28]. The Nd(III) center is nine coordinate having distorted tricapped trigonal prism geometry around the Nd^{III}. The nine coordination positions of the Nd^{III} is satisfied by three nitrogen centers of a terpyridyl ligand, three oxygen centers of three DMF molecule, two bridging cyano nitrogens, and methanol oxygen.

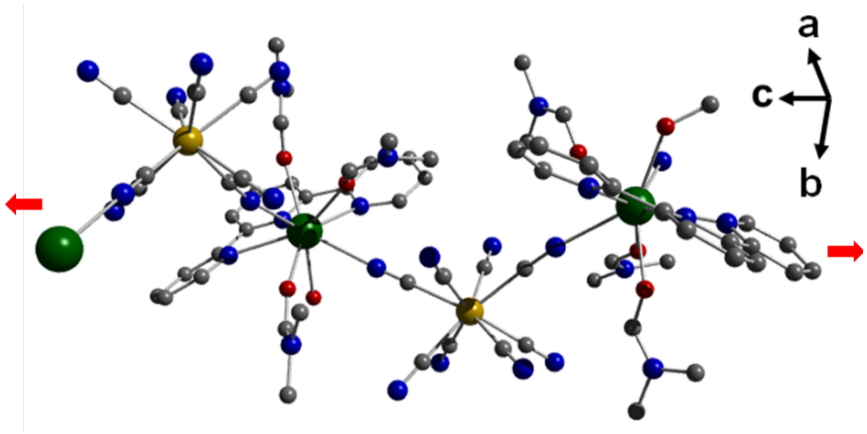

Fig. 2. Perspective view of the 1-D chain in Complex NdMo-1. Hydrogen atoms and lattice MeOH have been omitted for clarity.

The two DMF oxygens O1, O3, and a terpyridyl nitrogen N4 forms one trigonal face, while methanol oxygen O4, DMF oxygen O2, and terpyridyl nitrogen N6 generate another trigonal face. The two bridging cyano nitrogens N11 and N14, as well as the third terpyridyl nitrogen N5, are lying on three rectangular faces of the trigonal prism units. The separation between the Mo^{V} and Nd^{III} center is 5.91 Å. A distinction in the distances for the Nd–N bonds to the octacyanometalate groups and to the terpyridine moiety is evident. The Nd–N bonds to the latter are longer by approximately 0.034 Å on an average, which was also reported by Muddassir *et al.* using similar kinds of materials (Muddassir *et al.*, 2013). Eight cyanide groups coordinate the Mo^{V} ion with Mo–C distance averages of 2.168 (5) Å, consistent with reported structural studies on octacyanomolybdate-based complexes (Tong *et al.*, 2013).

The supramolecular architecture of Complex NdMo-1 is stabilized by several inter- and intramolecular non-covalent interactions. Amongst the intermolecular interactions, the important is the hydrogen bonding N···H and O···H interactions; besides, the other weak Nd···N and O···N interactions (Figs. 3A) also stabilizes the structure in solid-state. The intramolecular hydrogen bonding N···H interactions operate between H6B and N7 centers with H6B···N7 interaction distance 2.516 Å with ∠C6-H6B···N7 of 129.28°. Also, another N···H interaction between H8C and N9 operates with interaction distance 2.725 Å and ∠C8-H8C···N9 of 131.77°. Besides, the O···H interactions also operate between the DMF oxygen O1 and H13 hydrogen of the aromatic terpyridyl moiety with an interaction distance of 2.924 Å and ∠C18-H18···O1 of 164.69° (Fig. 3b). In comparison to the N···H interactions, the O···H interactions are relatively more linear and hence are more stable than the N···H interactions. Apart from the intermolecular interactions, intramolecular O···H hydrogen bonding also occurs between H2C and O1 centers with H2C···O1 interaction distance 2.344 Å with ∠C6-H2C···O1 of 105.55°, which is further assisted by another H9C···O3 hydrogen bonding with interaction distance of 2.405 Å and ∠C9-H9C···O3 of 104.61° (Fig. S1).

In addition to the interactions mentioned above, an unusual type of supramolecular interaction N···O exists between the oxygen center of lattice solvent methanol molecule with cyano nitrogen (Fig. S2). The N12···O19 interaction distance is 2.838 Å while the ∠C12-N12···O19 is 151.40° and N13···O4 interaction distance is 2.791 Å with ∠C13-N13···O4 of 163.09°. These unusual non-covalent interactions possess dimensions more significant than the sum of their covalent radii but less than the sum of their Van der Waals's radii ($\sum_{RvdW}$= 3.07 Å).

3.2 Hirshfeld surface analyses and fingerprint plots

Hirshfeld Surface Analyses is paramount importance to define the space occupied by a molecule in a crystal to partition the crystal electron density into molecular fragments (McKinnon *et al.*, 2007; Shi *et al.*, 2019; M. A. Spackman & Jayatilaka, 2009; M. A. Spackman *et al.*, 2008; P. R. Spackman *et al.*, 2016; Turner, Grabowsky *et al.*, 2014; Turner *et al.*, 2015; Woińska *et al.*, 2014).

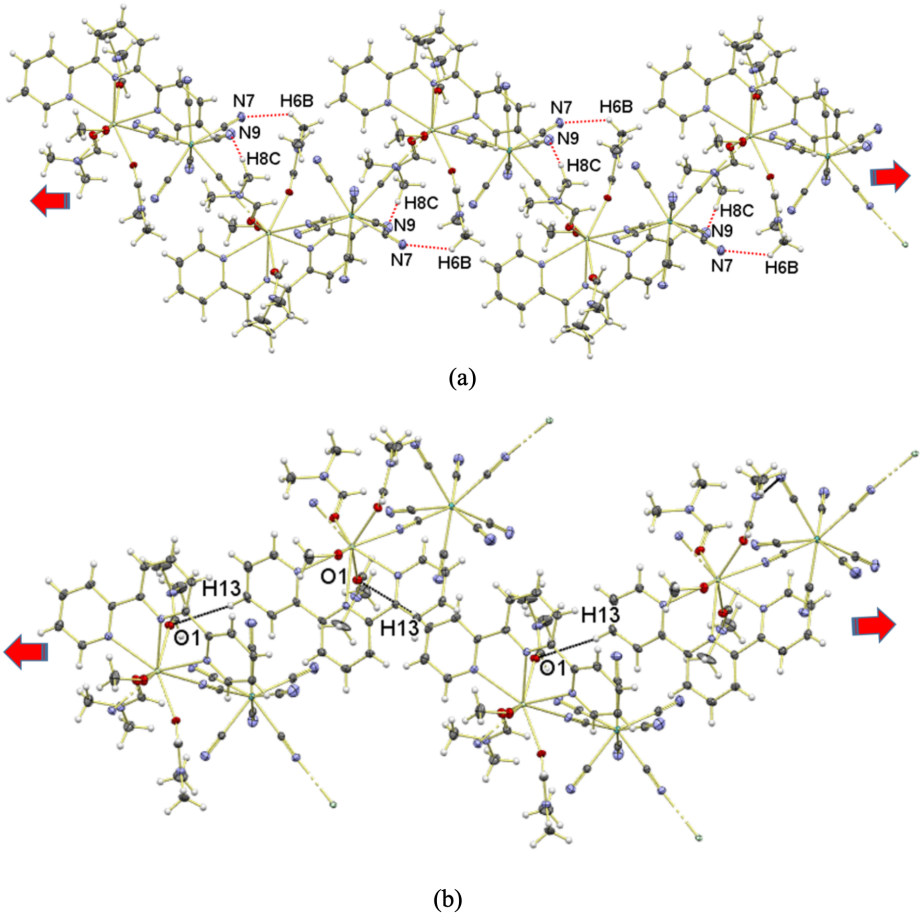

Fig. 3. (a) The N···H hydrogen bonding interactions operating in Complex NdMo-1; (b) The O···H hydrogen bonding interactions are operating in Complex NdMo-1.

The Hirshfeld surface for the complex is presented in Figure 5, showing surfaces that have been mapped over a d_{norm} range of -0.504 to 1.593 Å. The surfaces are shown as transparent to allow visualization of the aromatic rings and other moieties around which they were calculated. The weak interaction information discussed in the X-ray crystallography section is summarized adequately in the spots, with the large circular depressions (deep red) visible on the d_{norm} surfaces indicative of hydrogen bonding contacts. The dominant interactions between C−O···H and C−N···H for the complex can be seen in Hirshfeld surface plots as the red shaded area in Figure 5. Along with these deep red depressions, small area and light color on the surface indicates weaker and longer contact other than hydrogen bonds. Also, craters in the d_{norm} represent the H···H contacts. The surface curvedness which is constructed between -4 to 0.4 Å is a measure of the shape and area having very sharp curvatures that provide information regarding the nature of weak interactions. Blue patches evince the large surface curvedness while the areas with flat or subtle curvatures are evidenced by low surface curvedness. The surface curvedness plot for the complex reveals that all the interactions do not exhibit similar strength and hence are not isoenergetic in nature (He *et al*., 2019). This may be the reason because of which the Hirshfeld curvedness surface is relatively less flattened and more curved with blue and blue-green patches.

Using Hirshfeld surface data, the entire fingerprint plot had also been constructed, which had further been decomposed to obtain the relative contribution (in percentage) for different interaction (Fig. 4) existing in the crystal structure of the complex. Like d_{norm}, in the fingerprint plot too, the presence of spikes is indicative of robust C-O···H and C-N···H hydrogen bonding interactions.

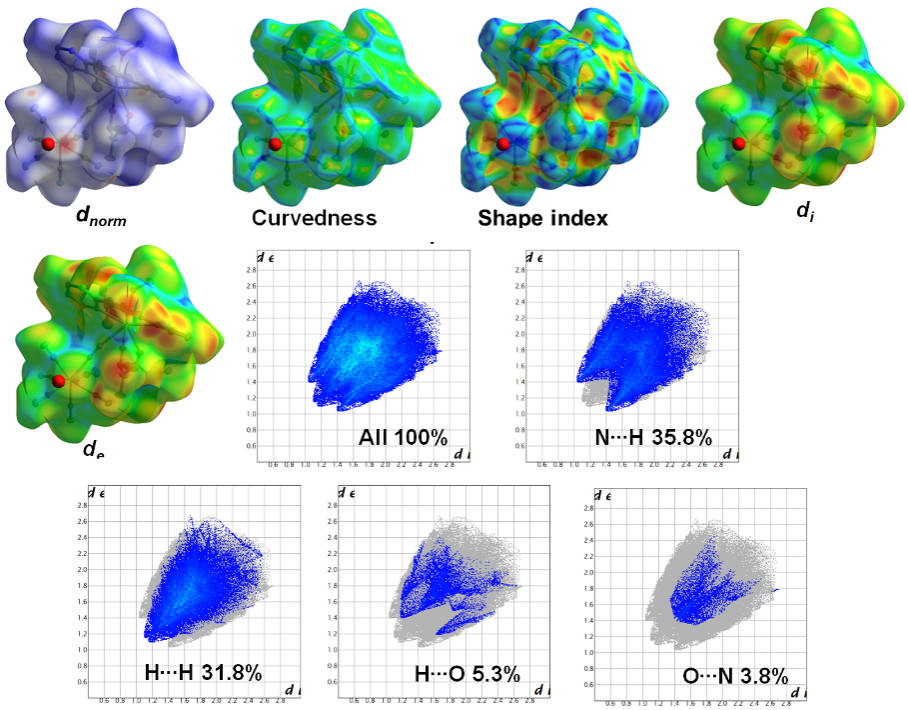

Fig. 4. Hirshfeld surface analyses and fingerprint plots of Complex NdMo-1.

The decomposed fingerprint plots indicate that the N···H intramolecular hydrogen bonding interactions contribute by 35.8%, while O···H intramolecular hydrogen bonding offers a 5.3% contribution in the total Hirshfeld surface. Also, the unusual O···N interactions contribute by 3.8% in the total Hirshfeld surface coverage (Fig. 4). Besides, the Hirshfeld surface analysis for the complex shows that H···H contacts make up 31.8% of the total Hirshfeld surface. This high proportion of H···H interactions may be arising because of the presence of aromatic hydrogens of the terpyridyl moiety and aliphatic hydrogens of the coordinated DMF and methanol.

Using Hirshfeld surface data, the entire fingerprint plot had also been constructed, which had further been decomposed to obtain the relative contribution (in percentage) for different interaction (Fig. 4) existing in the crystal structure of the complex. Like d_{norm}, in the fingerprint plot too, the presence of spikes is indicative of robust C-O···H and C-N···H hydrogen bonding interactions. The decomposed fingerprint plots indicate that the N···H intramolecular hydrogen bonding interactions contribute by 35.8%, while O···H intramolecular hydrogen bonding offers a 5.3% contribution in the total Hirshfeld surface. Also, the unusual O···N interactions contribute by 3.8% in the total Hirshfeld surface coverage (Fig. 4). Besides, the Hirshfeld surface analysis for the complex shows that H···H contacts make up 31.8% of the total Hirshfeld surface. This high proportion of H···H interactions may be arising because of the presence of aromatic hydrogens of the terpyridyl moiety and aliphatic hydrogens of the coordinated DMF and methanol.

Conclusions

New octacyanomolybdate-based Nd(III) complex (NdMo-1) has been successfully synthesized in the presence of terpyridine, and structurally characterized which results in the formation of alternating bridging cyanide ligands, i.e., the compounds consist of 1-D chains where Mo(V) and Nd(III) metal ions are linked in an alternating fashion. This architecture forms a single strand helically chiral topology with P (Δ) configuration. Corresponding chains are connected utilizing hydrogen bond interactions to form a three-dimensional supramolecular structure that stabilizes the whole molecule. However, DMF molecules are not involved in any H-bonding interactions.

These interactions have been validated using the Hirshfeld surface analysis. Due to the availability

of a significant number of hydrogen atoms in the compound and because of the non-planarity in molecular geometry, several hydrogen atoms fall at a distance of less than the sum of their Van der Waals radii, thereby taking an active part in inducing stability to the supramolecular architecture and thus stabilized the whole molecule. The reported complex and similar types of such complexes are suitable for the construction of magnetic materials that may be investigated further for properties such as quantum computing and information storage. We expect that further research on these types of materials will evolve in the direction of advanced multifunctional materials.

Acknowledgements

I am grateful to Researchers Supporting Project Number (RSP-2019/141), King Saud University, Riyadh, Saudi Arabia, for financial assistance.

References

Bok, L. D. C., Leipoldt, J. G., & Basson, S. S. (1975). The preparation of $Cs_3Mo(CN)_8 \cdot 2H_2O$ and $Cs_3W(CN)_8 \cdot 2H_2O$. *Zeitschrift Für Anorganische Und Allgemeine Chemie 415*, 81-83. https://doi.org/10.1002/zaac.19754150111

Chelebaeva, E., Larionova, J., Guari, Y., Ferreira, R. A. S., Carlos, L. D., Paz, F. A. A., ... Guérin, C. (2009). Luminescent and magnetic cyano-bridged coordination polymers containing 4d-4f ions: toward multifunctional materials. *Inorganic Chemistry 48*, 5983-5995. https://doi.org/10.1021/ic900378d

Chelebaeva, E., Larionova, J., Guari, Y., Sá Ferreira, R. A., Carlos, L. D., Almeida Paz, F. A., ... Guérin, C. (2008). A luminescent and magnetic cyano-bridged Tb^{3+}-Mo^{5+} coordination polymer: toward multifunctional materials. *Inorganic Chemistry 47*, 775-777. https://doi.org/10.1021/ic702192k

Chorazy, S., Nakabayashi, K., Ohkoshi, S., & Sieklucka, B. (2014). Green to red luminescence switchable by excitation light in cyanido-bridged TbIII-WV ferromagnet. *Chemistry of Materials 26*, 4072-4075. https://doi.org/10.1021/cm501954e

Chorazy, S., Rams, M., Nakabayashi, K., Sieklucka, B., & Ohkoshi, S. (2016). White light emissive DyIII single-molecule magnets sensitized by diamagnetic $[CoIII(CN)_6]^{3-}$ linkers. *Chemistry - A European Journal 22*, 7371-7375. https://doi.org/10.1002/chem.201601244

Chorazy, S., Rams, M., Wyczesany, M., Nakabayashi, K., Ohkoshi, S., & Sieklucka, B. (2018). Antiferromagnetic exchange and long-range magnetic ordering in supramolecular networks constructed of hexacyanido-bridged LnIII(3-pyridone)-CrIII (Ln = Gd{,} Tb) chains. *CrystEngComm 20*, 1271-1281. https://doi.org/10.1039/C7CE02077E

Chorazy, S., Wyczesany, M., & Sieklucka, B. (2017). Lanthanide Photoluminescence in Heterometallic Polycyanidometallate-Based Coordination Networks. *Molecules 22*, 1902. https://doi.org/10.3390/molecules22111902

Gao, Y., Viciano-Chumillas, M., Toader, A. M., Teat, S. J., Ferbinteanu, M., & Tanase, S. (2018). Cyanide-bridged coordination polymers constructed from lanthanide ions and octacyanometallate building-blocks. *Inorg. Chem. Front. 5*, 1967-1977. https://doi.org/10.1039/C8QI00357B

Goodwin, A. L., Calleja, M., Conterio, M. J., Dove, M. T., Evans, J. S. O., Keen, D. A., ... Tucker, M. G. (2008). Colossal Positive and Negative Thermal Expansion in the Framework Material $Ag_3[Co(CN)_6]$. *Science 319*, 794-797. https://doi.org/10.1126/science.1151442

He, J., Wang, J., Xu, Q., Wu, X., Dutta, A., Kumar, A., ... Abduh, N. A. Y. (2019). Syntheses and crystal structures of new dinuclear lanthanide complexes based on 3-(4-hydroxyphenyl)propanoic acid: Hirshfeld surface analyses and photoluminescence sensing. *New J. Chem. 43*, 13499-13508. https://doi.org/10.1039/C9NJ02213A

Hendrickx, M. F. A., Mironov, V. S., Chibotaru, L. F., & Ceulemans, A. (2004). Assignment of the Electronic Spectra of $[Mo(CN)_8]^{4-}$ and $[W(CN)_8]$4- by Ab Initio Calculations. *Inorganic Chemistry 43*, 3142-3150. https://doi.org/10.1021/ic035282t

Kaes, C., Hosseini, M. W., Rickard, C. E. F., Skelton, B. W., & White, A. H. (1998). Synthesis and Structural Analysis of a Helical Coordination Polymer Formed by the Self-Assembly of a 2,2'-Bipyridine-Based exo-Ditopic Macrocyclic Ligand and Silver Cations. *Angewandte Chemie International Edition 37*, 920-922. https://doi.org/10.1002/(SICI)1521-3773(19980420)37:7<920::AID-ANIE920>3.0.CO;2-O

Kaye, S. S., & Long, J. R. (2005). Hydrogen Storage in the Dehydrated Prussian Blue Analogues $M_3[Co(CN)_6]_2$ (M = Mn, Fe, Co, Ni, Cu, Zn). *Journal of the American Chemical Society 127*, 6506-6507.https://doi.org/10.1021/ja051168t

Kumar, A., Hüch, V., & Ram, V. J. (2013). Partially reduced thiochromene based oxathiahelicenes: crystallographic{,} computational and Hirschfeld surface analyses. *CrystEngComm 15*, 7019-7030.https://doi.org/10.1039/C3CE41078A

Ma, S.-L., Ren, S., Ma, Y., & Liao, D.-Z. (2009). Sheet-like of MoV-SmIII assembly containing $[MoV(CN)_8]^{3-}$ and Sm^{3+} ions as building blocks. *Journal of Chemical Sciences 121*, 421-427. https://doi.org/10.1007/s12039-009-0049-0

Ma, S.-L., Ren, S., Ma, Y., Liao, D.-Z., & Yan, S.-P. (2010). A Novel Bimetallic Chain Based on $[Mo(CN)_8]^{3-}$ and Yb^{3+} Ions as Building Blocks in Which Containing Many Intriguing Structural Features. *Journal of Inorganic and Organometallic Polymers and Materials 20*, 229-234. https://doi.org/10.1007/s10904-010-9359-4

McKinnon, J. J., Jayatilaka, D., & Spackman, M. A. (2007). Towards quantitative analysis of intermolecular interactions with Hirshfeld surfaces. *Chem. Commun. 37*, 3814-3816. https://doi.org/10.1039/B704980C

Muddassir, M., Song, X.-J., Chen, Y., Cao, F., Wei, R.-M., & Song, Y. (2013). Ion-induced diversity in structure and magnetic properties of hexacyanometalate-lanthanide bimetallic assemblies. *CrystEngComm 15*, 10541-10549. https://doi.org/10.1039/C3CE41704B

Nowicka, B., Korzeniak, T., Stefańczyk, O., Pinkowicz, D., Chorązy, S., Podgajny, R., & Sieklucka, B. (2012). The impact of ligands upon topology and functionality of octacyanidometallate-based assemblies. *Coordination Chemistry Reviews 256*, 1946-1971. https://doi.org/https://doi.org/10.1016/j.ccr.2012.04.008

Ohkoshi, S., Imoto, K., Tsunobuchi, Y., Takano, S., & Tokoro, H. (2011). Light-induced spin-crossover magnet. *Nature Chemistry 3*, 564-569. https://doi.org/10.1038/nchem.1067

Prins, F., Pasca, E., de Jongh, L. J., Kooijman, H., Spek, A. L., & Tanase, S. (2007). Long-range magnetic ordering in a TbIII-MoV cyanido-bridged quasi-one-dimensional complex. *Angewandte Chemie International Edition 46*, 6081-6084. https://doi.org/10.1002/anie.200701847

Qian, S.-Y., Zhou, H., Yuan, A.-H., & Song, Y. (2011). Syntheses, structures, and magnetic properties of five novel octacyanometallate-based lanthanide complexes with helical chains. *Crystal Growth & Design 11*, 5676-5681. https://doi.org/10.1021/cg201217a

SAINT, V. (2014). 8.34 A. Bruker AXS. Inc., Madison, Wisconsin, USA.

Sato, O., Iyoda, T., Fujishima, A., & Hashimoto, K. (1996). Photoinduced magnetization of a cobalt-iron cyanide. *Science 272*, 704-705. https://doi.org/10.1126/science.272.5262.704

Sheldrick, George M. (2015). Crystal structure refinement with SHELXL. *Acta Crystallographica. Section C, Structural Chemistry 71*, 3-8. https://doi.org/10.1107/S2053229614024218

Shen, H. (2014). The synthesis, crystal structure and magnetic properties of a one-dimensional terbium(III){–}octa{-}cyanido{-}molybdate(V) assembly. *Acta Crystallographica Section C 70*, 1169-1173. https://doi.org/10.1107/S2053229614024085

Shi, M. W., Thomas, S. P., Hathwar, V. R., Edwards, A. J., Piltz, R. O., Jayatilaka, D., ... Spackman, M. A. (2019). Measurement of electric fields experienced by urea guest molecules in the 18-crown-6/urea (1:5) host-guest complex: an

experimental reference point for electric-field-assisted catalysis. *Journal of the American Chemical Society 141*, 3965-3976. https://doi.org/10.1021/jacs.8b12927

Spackman, M. A., & Jayatilaka, D. (2009). Hirshfeld surface analysis. *CrystEngComm 11*, 19-32. https://doi.org/10.1039/B818330A

Spackman, M. A., McKinnon, J. J., & Jayatilaka, D. (2008). Electrostatic potentials mapped on Hirshfeld surfaces provide direct insight into intermolecular interactions in crystals. *CrystEngComm 10*, 377-388. https://doi.org/10.1039/B715227B

Spackman, P. R., Thomas, S. P., & Jayatilaka, D. (2016). High throughput profiling of molecular shapes in crystals. *Scientific Reports 6*, 22204. https://doi.org/10.1038/srep22204

Tanase, S., Evangelisti, M., de Jongh, L. J., Smits, J. M. M., & de Gelder, R. (2008). Crystal structure, magnetic and thermal properties of the one-dimensional complex $[Nd(pzam)_3(H_2O)Mo(CN)_8]\cdot H_2O$. *Inorganica Chimica Acta 361*, 3548-3554. https://doi.org/https://doi.org/10.1016/j.ica.2008.03.026

Tanase, S., Ferbinteanu, M., & Cimpoesu, F. (2011). Rationalization of the lanthanide-ion-driven magnetic properties in a series of 4f-5d cyano-bridged chains. *Inorganic Chemistry 50*, 9678-9687. https://doi.org/10.1021/ic201427w

Tanase, S., Mittelmeijer-Hazeleger, M. C., Rothenberg, G., Mathonière, C., Jubera, V., Smits, J. M. M., & de Gelder, R. (2011). A facile building-block synthesis of multifunctional lanthanide MOFs. *J. Mater. Chem. 21*, 15544-15551. https://doi.org/10.1039/C1JM12789F

Tong, Y.-Z., Wang, Q.-L., Su, C.-Y., Ma, Y., Ren, S., Xu, G.-F., ... Liao, D.-Z. (2013). Nine cyanide-bridged bimetallic magnetic chains derived from octacyanomolybdate(v) and lanthanide(iii) building blocks. *CrystEngComm. 15*, 9906-9915. https://doi.org/10.1039/C3CE41048J

Turner, M. J., Grabowsky, S., Jayatilaka, D., & Spackman, M. A. (2014). Accurate and efficient model energies for exploring intermolecular interactions in molecular crystals. *The Journal of Physical Chemistry Letters 5*, 4249-4255. https://doi.org/10.1021/jz502271c

Turner, M. J., Thomas, S. P., Shi, M. W., Jayatilaka, D., & Spackman, M. A. (2015). Energy frameworks: insights into interaction anisotropy and the mechanical properties of molecular crystals. *Chem. Commun. 51*, 3735-3738. https://doi.org/10.1039/C4CC09074H

Wang, J., Zhang, Z.-C., Wang, H.-S., Kang, L.-C., Zhou, H.-B., Song, Y., & You, X.-Z. (2010). Eicosanuclear Cluster [Cu13W7] of copper-octacyanotungstate bimetallic assembly: synthesis, structure, and magnetic properties. *Inorganic Chemistry 49*, 3101-3103. https://doi.org/10.1021/ic100282w

Wang, X.-Y., Prosvirin, A. V, & Dunbar, K. R. (2010). A docosanuclear Mo_8Mn_{14} cluster based on $[Mo(CN)_7]^{4-}$. *Angewandte Chemie International Edition 49*, 5081-5084. https://doi.org/10.1002/anie.201001664

Wang, Z.-X., Shen, X.-F., Wang, J., Zhang, P., Li, Y.-Z., Nfor, E. N., ... You, X.-Z. (2006). A sodalite-like framework based on octacyanomolybdate and neodymium with guest methanol molecules and neodymium octahydrate ions. *Angewandte Chemie International Edition 45*, 3287-3291. https://doi.org/10.1002/anie.200600455

Wang, Z.-X., Zhang, P., Shen, X.-F., Song, Y., You, X.-Z., & Hashimoto, K. (2006). Syntheses, structures, and properties of two three-dimensional octacyanometalate-based polymers: $Cs_2Cu_3[W(CN)_8]_2\cdot 4NH_3\cdot 4H_2O$ and $Cu_2[Mo(CN)_8]\cdots 8NH_3$. *Crystal Growth & Design 6*, 2457-2462. https://doi.org/10.1021/cg050555b

Woińska, M., Jayatilaka, D., Spackman, M. A., Edwards, A. J., Dominiak, P. M., Woźniak, K., ... Grabowsky, S. (2014). Hirshfeld atom refinement for modelling strong hydrogen bonds. *Acta Crystallographica Section A 70*, 483-498. https://doi.org/10.1107/S2053273314012443

Yadav, R., Trivedi, M., Kociok-Köhn, G., Prasad, R., & Kumar, A. (2015). New

Ni(ii) 1{,}2-bis(diphenylphosphino)ethane dithiolates: crystallographic{,} computational and Hirshfeld surface analyses. *CrystEngComm 17*, 9175-9184. https://doi.org/10.1039/C5CE01526J

Yuan, A.-H., Lu, R.-Q., Zhou, H., Chen, Y.-Y., & Li, Y.-Z. (2010). Three unique two-fold interpenetrated three-dimensional networks with PtS-type topology constructed from $[M(CN)_4]_2$- (M = Ni{,} Pd{,} Pt) as "square-planar" building blocks. *CrystEngComm 12*, 1382-1384. https://doi.org/10.1039/B917262A